Macromolecular Bioscience
www.mbs-journal.de

Unlocking Novel Anticancer Strategies: Bioactive Hydrogels for Local Delivery of Plasma-Derived Oxidants in an In Ovo Cancer Model

Albert Espona-Noguera, Milica Živanić, Evelien Smits, Annemie Bogaerts, Angela Privat-Maldonado, and Cristina Canal**

Cold atmospheric plasma (CAP) is a tool with the ability to generate reactive oxygen and nitrogen species (RONS), which can induce therapeutic effects like disinfection, wound healing, and cancer treatment. In the plasma oncology field, CAP-treated hydrogels (PTHs) are being explored for the local administration of CAP-derived RONS as a novel anticancer approach. PTHs have shown anticancer effects in vitro, however, they have not yet been studied in more relevant cancer models. In this context, the present study explores for the first time the therapeutic potential of PTHs using an advanced in ovo cancer model. PTHs composed of alginate (Alg), gelatin (Gel), Alg/Gel combination, or Alg/hyaluronic acid (HA) combination are investigated. All embryos survived the PTHs treatment, suggesting that the in ovo model could become a time- and cost-effective tool for developing hydrogel-based anticancer approaches. Results revealed a notable reduction in CD44+ cell population and their proliferative state for the CAP-treated Alg-HA condition. Moreover, the CAP-treated Alg-HA formulation alters the extracellular matrix composition, which may help combat drug-resistance. In conclusion, the present study validates the utility of in ovo cancer model for PTHs exploration and highlights the promising potential of Alg-based PTHs containing HA and CAP-derived RONS for cancer treatment.

1. Introduction

Cold atmospheric plasma (CAP) is a partially ionized gas that has found wide applications in biomedicine, from wound healing to cancer treatment.[1] This is because plasma represents an exogenous source of RONS that play an important role in cell physiology and pathology. In high concentrations, CAP-derived RONS induce irreversible damage and cell death.[2] Due to the imbalance of reactive oxygen and nitrogen species (RONS) formation and removal in cancer cells, they accumulate more RONS than non-malignant cells. The characteristic oxidative stress state of cancer cells plays a significant role in the hallmarks of cancer, and makes them more sensitive than normal cancer cells to pro-oxidant therapies, such as CAP.[3]

Besides direct CAP treatment, where the target is exposed directly to a CAP source (usually a DBD device or a CAP jet),[4] indirect treatments are also possible via the administration of a CAP-treated solution.

A. Espona-Noguera, M. Živanić, C. Canal
Biomaterials
Biomechanics
and Tissue Engineering Group
Department of Materials Science and Engineering and Research Centre for Biomedical Engineering
Universitat Politècnica de Catalunya
BarcelonaTech (UPC)
Av. Eduard Maristany 10–14, Barcelona 08019, Spain
E-mail: cristina.canal@upc.edu

A. Espona-Noguera, M. Živanić, C. Canal
Barcelona Research Center in Multiscale Science and Engineering
Universitat Politècnica de Catalunya
BarcelonaTech (UPC)
Barcelona 08019, Spain

The ORCID identification number(s) for the author(s) of this article can be found under https://doi.org/10.1002/mabi.202400213

DOI: 10.1002/mabi.202400213

M. Živanić, A. Bogaerts, A. Privat-Maldonado
Plasma Lab for Applications in Sustainability and Medicine-Antwerp (PLASMANT)
Department of Chemistry
University of Antwerp
Antwerp 2610, Belgium
E-mail: angela.privatmaldonado@uantwerpen.be

E. Smits
Center for Oncological Research
Integrated Personalized and Precision Oncology Network
University of Antwerp
Antwerp 2610, Belgium

C. Canal
Centro de Investigación Biomédica en Red de Bioingeniería
Biomateriales y Nanomedicina
Instituto de Salud Carlos II
Barcelona 28029, Spain

The latter allows for minimally invasive and repeated treatment of internal tumors. In indirect treatments, a solution is first treated with CAP to enrich it with long-lived RONS and is then administered to the target (e.g., via injection). In other words, the solution acts as a vehicle for the delivery of CAP-derived oxidants. This solution can be a liquid (CAP-treated liquid, PTL),[5] or a polymeric solution that is later crosslinked into a hydrogel (CAP-treated hydrogel, PTH).[6,7] Compared to PTLs, which are easily washed away and diluted by different body fluids, PTHs can be locally administered to the target tissue, thus enabling controlled delivery of RONS. In addition, PTHs present a more complex system that could enable more varied CAP chemistry and biological effects. For example, different chemical groups of polymers could interact with CAP to produce organic peroxides or favor the production of a certain subset of RONS (e.g., nitrogen species).[8,9]

Due to their unique properties, hydrogels are broadly used for regenerative medicine and controlled drug delivery.[10,11] Hydrogels are 3D networks of crosslinked hydrophilic polymers and water, with a porous microstructure and viscoelastic properties that make them mechanistically similar to the extracellular matrix (ECM) of tissues. The rich chemistry of polymers allows to fine-tune the chemical properties of the hydrogel to design biocompatible, biodegradable, and bioactive hydrogels that can be used in clinics. Polymers can be of natural origin (biopolymers) or synthesized in laboratories. While the latter enables better control over physicochemical properties and polymer homogeneity, the first offers a time- and cost-effective alternative, as they are commercially available and inherently biocompatible.[12] Alginate (Alg) is a commonly used biopolymer in biomedical engineering thanks to many favorable properties and great versatility. Namely, Alg is a non-immunogenic, biocompatible and biodegradable polysaccharide extracted from brown algae, that is biologically inert but can be easily functionalized (chemically modified) or combined with other components to achieve different hydrogel properties,[13,14] for example, to improve adhesion of cells. In addition, Alg crosslinks in the presence of divalent cations (e.g., Ca^{2+}), making the preparation of Alg hydrogels straightforward. In this sense, Alg can be used as a basis for hydrogel preparation, and further, more bioactive, polymers can be included in the gel that normally would not crosslink on their own, but would require chemical modifications or more complex crosslinking strategies. Gelatin (Gel) is a polypeptide that is derived from collagen, the main component of connective tissues.[15] As such, it improves the bioactivity and mechanical strength of a hydrogel. Hyaluronic acid (HA) is another component abundantly present in the ECM of tissues. It is a polysaccharide that mainly has a hydrating role but can also interact with cell receptors involved in different signaling cascades, for example, cell proliferation and migration.[16]

Previously, we explored the application of PTHs in vitro, showing that the inclusion of bioactive polymers (HA in particular) within Alg PTH can improve its selective cytotoxicity, eliminating osteosarcoma cells but not human mesenchymal stem cells, which survive and proliferate well after treatment.[17] However, while good for initial characterization and screening of therapies, 2D cell culture models are of poor clinical relevance.[18] 3D cell culture models such as spheroids or scaffold-based models mimic the solid tumors better and can already alter the expression of genes and the response of cancer cells to the treatment compared to 2D.[19] A more cost- and time-efficient alternative to traditional mouse models is the in ovo model, where fertilized chicken eggs are used to generate small tumors on the chick chorioallantoic membrane (CAM). As chicken embryos lack a functional immune system, they can be considered an immunodeficient host. This allows the implantation of foreign cells without any species-specific restrictions. The CAM is highly vascularized and shares different ECM components found in humans (e.g., fibronectin, collagen, and matrix metalloproteinases), making it a great model to study angiogenesis, tumor invasion, and even metastasis.[20,21]

In this study, we used the pancreatic cancer in ovo model to characterize different Alg-based PTHs for cancer therapy. PTHs are a newly proposed concept and so far, there is a limited number of in vitro[6,7,17,22] and in vivo studies.[23] Thus, the aim of this work was to evaluate the suitability of the in ovo model for studying PTHs and to assess the therapeutic effects of CAP-derived RONS delivered via PTHs. Since polymer chemistry influences the generation of RONS and the bioactivity of hydrogel, PTHs of different compositions (Alg, Gel, Alg + Gel, and Alg + HA) were compared. Since the HA employed in the present study does not have the ability to crosslink by itself, it was only evaluated in combination with Alg. Different aspects of the tumor were observed, for example, weight and composition, proliferative state of cancer cells, composition of ECM, among others. Our results provide an important basis for further research and development of PTH-based therapies using the clinically relevant in ovo model.

2. Experimental Section

2.1. Cell Lines and Reagents

The human pancreatic cancer cell line Mia PaCa-2 was obtained from Service GmbH. Cells were grown in Dulbecco's modified Eagle medium (Gibco) supplemented with 10% fetal bovine serum (Gibco), 2 mM L-glutamine (Life Technologies), 100 U mL^{-1} penicillin, and 100 µg mL^{-1} streptomycin (Gibco). Cell cultures were maintained at 37 °C and 5% CO_2, and detached using Trypsin-EDTA (0.05%, Gibco).

The following biopolymers were used to generate hydrogels: sodium alginate (M_W: 10–600 KDa, 99.8%, Panreac), Dermial,[24] a commercial product composed mainly by hyaluronic acid (M_W: 1.3 MDa, 60–75%) kindly provided by Bioiberica S.A.U., and bovine skin gelatin (M_W: 40–50 KDa, ≥95%, Sigma-Aldrich). The crosslinking solution was a mixture of disodium hydrogen phosphate dihydrate ($Na_2HPO_4{\cdot}2H_2O$, M_W: 177,99 g mol^{-1}, >98.0%, Fluka), and calcium sulphate dihydrate ($CaSO_4{\cdot}2H_2O$. M_W: 172.17 g mol^{-1}, 98.0%, Merck).

High-purity Argon gas (99.999%, Air Liquide) was used to generate CAP. Griess reagent employed for the detection of nitrites (NO_2^-) was prepared with phosphoric acid (H_3PO_4, M_W: 97994 g mol^{-1}, 85.0–88.0% w/w), sulphanilamide ($C_6H_8N_2O_2S$, M_W: 172.20 g mol^{-1}, ≥99%), and *N*-(1-naphthyl) ethylenediamine dihydrochloride ($C_{12}H_{16}Cl_2N_2$, M_W: 172.20 g mol^{-1}, >98%); all of them purchased from Panreac. Amplex Red (Invitrogen) and horseradish peroxidase type IV (HRP, Sigma-Aldrich) were used for the detection of hydrogen peroxide (H_2O_2). For the calibration curves of NO_2^- and H_2O_2, sodium nitrite ($NaNO_2$, M_W: 69.00 g

Table 1. Reagents used for immunohistochemistry.

	Reagent	Dilution	Clone	Cat. No.	Manufacturer
1° Abs	CD44			3570S	Cell Signaling Technology
	ki67	1/75	MIB-1	M724029-2	Dako
	cleaved caspase-3	1/200		9661S	Cell Signaling Technology
	p53	1/2	DO-7	GA616	Dako Omnis
	TrxR1	1/100	B-2	SC28321	Santa Cruz Biotechnology
	CA-9	1/350		ab10471	Abcam
2° Abs	Envision FLEX /HRP			DM842	Dako Omnis
	IgG (H+L) Alexa Fluor 594	1/500		A21203	Thermo Fisher
Additional reagents	EnVision FLEX+ Rabbit linker			K8009	Dako
	Wash buffer			S3006	Dako
	Donkey serum			ab7475	Abcam
	Goat serum			ab7481	Abcam
	VECTASHIELD HardSet antifade mounting medium with DAPI			H-1500-10	Vectorlabs

mol^{-1}, >98.0%), and H_2O_2 solution (M_W: 34.01 g mol^{-1}, 30% w/w) from Sigma-Aldrich were used, respectively.

For immunohistochemistry, the following reagents were used: Hematoxylin crystals (C.I. 75 290), Eosin Y disodium salt and Alcian Blue 8GX solution were obtained from Sigma-Aldrich, and Biebrich Scarlet (C.I. 26 905) from Hopkin and Willliams. Iron (III) chloride hexahydrate ($FeCl_3 \cdot 6H_2O$), fuchsin acid (C.I. 42 685), phosphomolybdic acid, phosphotungstic acid, and acetic acid 96% were purchased from Merck. Nuclear fast red solution was obtained from Carl Roth and Expert mounting medium from Cell Path. Full details of the primary and secondary antibodies and the additional reagents are reported in **Table 1**.

For the in ovo model, the following materials were used: 4-day old white leghorn chicken eggs (Kwekerij Wyverkens), diethyl ether (Fisher Scientific), growth factor-reduced Matrigel (8.6 mg mL^{-1}, Corning), Tegaderm plasters (3M Healthcare), silicone rings (Glasatelier), 0,9 mm × 40 mm needles (BD Microlance), filter paper (Tissue Tek II).

2.2. Generation of Biopolymer Solutions Treated with CAP

The multicomponent biopolymer formulations under study incorporating HA and Gel were prepared using a 0.25% Alg solution as base. First, sodium Alg powder was dissolved in sterile distilled water (dH_2O) by vortexing. Then, the different formulations were prepared by adding HA or Gel powder to the Alg solution at concentrations of 1% and 2%, respectively. Both biopolymers were dissolved using a heating orbital shaker at 37 °C at 200 rpm for 1 h. The 0.25% Alg and 2% Gel formulations were prepared following the same dissolution procedure. After complete dissolution, the biopolymer solutions were ready for treatment. The commercially available CAP jet kINPen IND (NEOPLAS Tools) was used. CAP was applied to 1 mL of the respective biopolymer solutions in a 24-well plate (Figure 1A). The treatment conditions were as follows: gas flow rate at 1 standard liter per min, 10 mm distance between the tip of the CAP nozzle and the surface of the solution, and treatment time of 10 min. The biopolymer solutions treated with CAP were then used for both RONS quantification and in ovo experiments. All steps were performed under sterile conditions.

2.3. Quantification of NO_2^- and H_2O_2

Colorimetric and fluorescence methods were used to quantify the concentration of NO_2^- and H_2O_2, respectively. For NO_2^-, the Griess reagent was prepared as described.[25] Briefly, 50 µL of each biopolymer solution treated with CAP were combined with 50 µL per well of Griess reagent and incubated for 10 min. The absorbance was measured at 540 nm using a Synergy Hybrid Multi-Mode Microplate Reader (Biotek Instruments). For H_2O_2, the Amplex Red/HRP reagent was used as described.[25] The CAP-treated biopolymer solutions were diluted 1:1000 in Milli-Q H_2O and mixed with 50 µL per well of Reagent Amplex Red/HRP reagent in a black 96-well plate. The samples incubated at 37 °C for 30 min light-protected, and subsequently, fluorescence intensity was measured using the same microplate reader at 560/20 nm for excitation and 590/20 nm for emission. The calibration curves for NO_2^- and H_2O_2 were obtained analyzing $NaNO_2$ and H_2O_2 standard solutions prepared into the corresponding biopolymer solution. For H_2O_2, standard solutions were prepared using biopolymer solution diluted 1:1000 in Milli-Q.

2.4. In Ovo Experiments

2.4.1. Tumor Generation on the CAM

For in ovo experiments, 4-day–old fertilized chicken eggs were positioned horizontally in the Ova-Easy 100 egg incubator (Brinsea) with automatic continuous rotation mode during 1 day at 37.7 °C and 65% humidity. One day after, the upper pole of the egg was disinfected, perforated with a 20G sterile needle, and sealed with medical tape to allow the repositioning of the air

sac. On day 7, 2×10^6 Mia PaCa-2 cells per egg were pelleted in 1.5 mL conical tubes and placed on ice until use. The egg shell was cut to expose the CAM, a filter paper soaked in diethyl ether was applied on a vascularized area of the CAM, and a sterile silicone ring (ID = 5 mm, ED = 6 mm) was placed in this region. The cell pellet was mixed with 20 µL of growth factor-reduced Matrigel, and loaded into the silicone ring. The eggs were sealed with Tegaderm (3D) and placed back in the incubator in vertical position. After 4 days (day 11), tumors were ready for treatment. All steps outside the incubator were carried out in sterility using a heat block set at 37.7 °C with a custom-made aluminum egg holder.

2.4.2. Formation of Hydrogels and Treatment of Tumors

Two different strategies were employed to form and apply the hydrogels for treatment of tumors. To prepare Gel hydrogels, 100 µL drops of CAP-treated Gel solution were pipetted on a petri dish, and then cooled at 4 °C to promote crosslinking, resulting in solid hydrogels that were stored in the fridge for <1 h before application on tumors. At this point, eggs were prepared for treatment. To this end, Tegaderm was cut to expose the tumor and a sterile plastic ring (ID = 7 mm, ED = 8.5 mm) was placed surrounding the tumor. Then, the different treatments were applied using hydrogels and dH_2O as control. The solid CAP-treated Gel hydrogels were directly placed into the ring, making direct contact with the tumor (one solidified Gel drop/egg). For Alg-based formulations, hydrogels were prepared and loaded onto the tumors in situ. Briefly, 150 µL of CAP-treated solution was mixed with 15 µL of the crosslinker (1:1 mixture of 2.44 M $CaSO_4$ and 125 mM $Na_2HPO_4{\cdot}2H_2O$) to initiate the crosslinking reaction. Subsequently, 100 µL of the mixture were loaded into the external ring, completely covering the exposed tumor surface. The procedure used for Alg-based formulations was also followed to apply the dH_2O control on tumors. After each treatment, the eggs were resealed with Tegaderm. All steps outside the incubator were carried out using a heat block (set at 37.7 °C) with a custom-made aluminum egg holder. The treatment procedure was performed daily for 3 days, with each egg receiving a total of 300 µL of CAP-treated dH_2O or hydrogels. Untreated samples of each formulation were used as controls. One day after the last treatment (day 14), images of the vasculature surrounding the tumor were collected, and then tumor tissues were extracted and weighed in a precision balance (Fisher). Finally, the tissues were processed for subsequent analysis.

2.5. Histological Staining

For all immunostainings, tissues were fixed with 4% paraformaldehyde and paraffin embedded. Sections of 5 µm were cut, deparaffinized and rehydrated prior to staining. Sections were imaged with a Zeiss AxioImager Z1 microscope (Carl Zeiss, Jena, Germany) equipped with an AxioCam MR v3.0. Whole slide imaging for hematoxylin and eosin was done with the Zeiss Axio Scan Z1Slide Scanner, with camera Hitachi HV-F203SCL.

2.5.1. Hematoxylin and Eosin

Slides were stained with hematoxylin solution for 2 min and rinsed with dH_2O for 2 min. After staining with eosin for 5 min, the slides were rinsed with dH_2O, dehydrated and mounted.

2.5.2. Masson's Trichrome

After deparaffinization and rehydration, the slides were stained with Weigert's hematoxylin for 10 min, washed again with tap H_2O for 10 min and rinsed in dH_2O. Next, the slides were stained with the Biebrich's scarlet fuchsin for 2 min, and rinsed in dH_2O. The slides were incubated in phosphotungstic-phosphomolybdic acid solution for 10–15 s and dyed with Light Green solution for 5 min. The slides were dehydrated and mounted.

2.5.3. Alcian Blue and Nuclear Fast Red

Slides were incubated in 3% acetic acid for 3 min, then stained in Alcian Blue for 30–45 min. After washing in running tap H_2O for 2 min, the slides were counterstained in Nuclear Fast Red for 3–5 min. The slides were washed again in running tap H_2O for 1 min, rinsed in dH_2O for 2 min, dehydrated and mounted.

2.5.4. Immunofluorescence Staining

Antigen retrieval was done with citrate buffer (10 mM, pH 6) for 20 min at 96 °C. The slides were washed twice in PBS with 0.3% Triton X-100 (PBST) for 5 min. Slides were blocked in PBST with 10% donkey serum for 2 h at RT. Slides were incubated overnight at 4 °C with anti-CD44 (1/400) diluted in TBST supplemented with 1% donkey serum. Slides were washed twice with PBST and incubated with the secondary antibody for 1 h at RT. Slides were washed twice and mounted with antifade mounting medium with DAPI.

2.5.5. Immunohistochemical Staining

Antigen retrieval was done for 20 min at 96 °C with citrate buffer (10 mM, pH 6) for Ki67 and cleaved caspase-3 or Tris/EDTA buffer (pH 9) for p53, TrxR1, and carbonic anhydrase 9 (CA-9). Endogenous peroxidases were blocked with 3% H_2O_2 in PBS (10 min, RT), followed by an incubation with 5% goat serum in wash buffer (S3006, Dako) supplemented with 0.1% Tween 20. Slides incubated with the primary antibody for 40–60 min at RT. An additional incubation for 15 min with the linker was done only for the slides stained for cleaved caspase-3 and CA-9. After washing the slides again, they were incubated with the secondary antibody (HRP) for 30 min. Finally, samples were incubated 5–10 min with diaminobenzidine to visualize positive cells and 2 min with hematoxylin to stain cell nuclei (counterstain).

2.6. Image Processing

Ki67, caspase-3, p-53, and TrxR1 immunohistochemistry scoring was done using QuPath (open-source software[26]). Positive cell

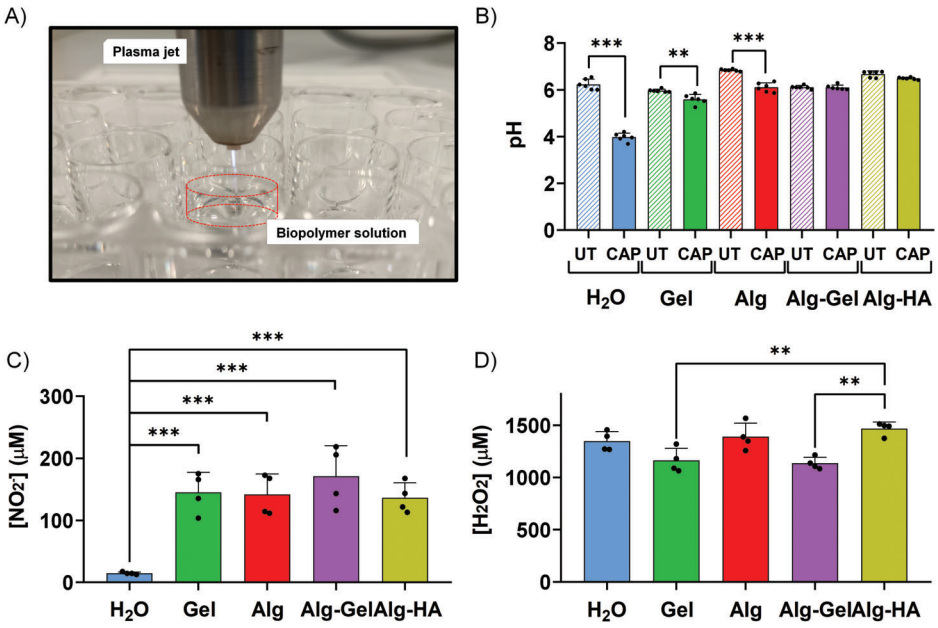

Figure 1. CAP treatment configuration for biopolymer solution and chemical characterization: pH and RONS quantification. A) CAP treatment of 1 mL of a biopolymer solution in a 24-well plate using the kINPen CAP jet. B) pH, C) NO_2^-, and D) H_2O_2 concentrations in dH_2O, 2% Gel, 0.25% Alg, 0.25% Alg–2% Gel, and 0.25% Alg–1% HA solution after 10-min CAP treatment. Each dot represents an independent sample measurement. Values represent mean ± SD. $^{**}p \leq 0.01$, $^{***}p \leq 0.001$.

detection was used with the following settings: detection image, optical density sum; requested pixel size, 0.5 µm; background radius, 8 µm; median filter radius, 0 µm; sigma, 1.5 µm; minimum cell area, 10 µm^2; maximum cell area, 400 µm^2; threshold, 0.1; maximum background; intensity, 2. The intensity threshold parameters were set as follows: 1+ = 0.2; 2+ = 0.4; 3+ = 0.6.

Whole slide images of tumor sections stained with hematoxylin and eosin (H&E) were analyzed in QuPath. Cell detection was used with the following settings: detection image, optical density sum; requested pixel size, 0.5 µm; background radius, 11 µm; median filter radius, 1 µm; sigma, 1.5 µm; minimum cell area, 10 µm^2; maximum cell area, 200 µm^2; threshold, 0.2; maximum background; intensity, 2. The object classifier was trained using seven training images to identify human cancer cells, stroma, CAM cells, red blood cells, and necrosis.

Images acquired for Masson's Trichrome and Alcian Blue were processed using ImageJ. After subtracting the background, the "color deconvolution" plugin for Masson's Trichrome was used, and the green component was identified as the collagen fibers. In the same way, Alcian Blue images were deconvoluted and the blue component was identified as the glycosaminoglycans (GAGs) fibers. The area of green collagen or GAGs fibers was masked using the "threshold" tool and the mask area was measured.

2.7. Blood Vessels Scoring

The number of blood vessels present in the tumor was counted manually by assessing three regions of interest of 200 × 200 µm in the core of the tumor and in the periphery (invasive front). For the macroscopical assessment, the CAM and tumors were imaged from the top. To macroscopically quantify the number of small and large blood vessels, two concentric circles (7 and 10 mm) were drawn and the number of intersecting blood vessels were counted twice independently, double-blinded.[27]

2.8. Statistical Analysis

Statistical analysis was carried out with GraphPad Prism v10.1.2. Data were presented as means ± standard deviation, and differences were considered significant for comparison of groups using one-way ANOVA, Tukey's post hoc test when $p \leq 0.05$.

3. Results

3.1. Quantification of RONS in Biopolymer Solutions

The effect of CAP on the pH of dH_2O and the hydrogels was monitored immediately after treatment. As expected, CAP-treated dH_2O presented a significant drop in the pH after 10 min of treatment ($p \leq 0.001$), whereas more modest reductions in pH values were observed in gelatin ($p \leq 0.01$) and alginate ($p \leq 0.001$; **Figure** 1B). The drop in pH in dH_2O was accompanied by significantly lower levels of NO_2^- (<30 µM) than those obtained in the CAP-treated hydrogels, which presented 140 µM NO_2^- in average (Figure 1C). For H_2O_2, we observed that both CAP-treated dH_2O and all the hydrogels contained more than 1000 µM H_2O_2, with Alg-HA being the hydrogel with the highest H_2O_2 concentration (Figure 1D). Altogether, these results indicate that CAP-treated hydrogels can retain significant amounts of NO_2^- and H_2O_2 without altering their pH even upon longer exposure to CAP.

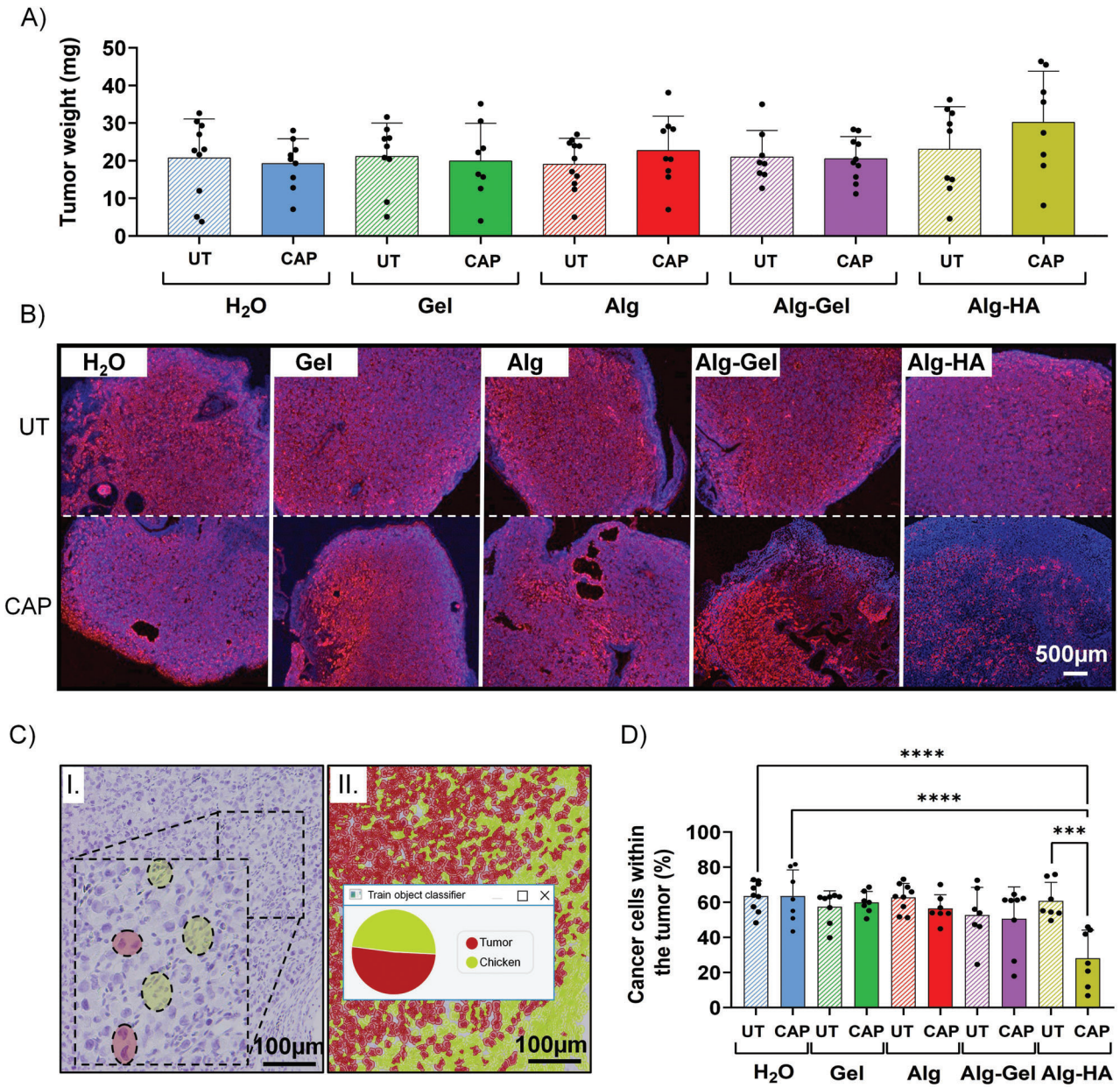

Figure 2. Evaluation of the tumor weight, and identification and segregation of the cellular subpopulations within the tumors. A) Weight of the collected tumors after three repeated exposures to dH_2O, 2% Gel, 0.25% Alg, 0.25% Alg–2% Gel, and 0.25% Alg–1% HA solutions treated with CAP for 10 min (CAP). Untreated (UT) sample for each condition was used as control. B) Immunofluorescence staining of CD44 marker to visualize the Mia PaCa-2 cells in red within the tumor sections. DAPI was used to visualize all nuclei in blue. Scale bar: 500 µm. C) Representative image of hematoxylin staining of tumor sections to visualize the nuclei of the cells; I) Mia PaCa-2 cancer cells highlighted in red and chicken cells highlighted in yellow. II) Identification and determination of the percentage of both cell populations present in the tumor sections using the cell classifier analysis from the QuPath software. Scale bar: 100 µm. D) Percentage of the cancer cells within the tumor after three repeated exposures to dH_2O, 2% Gel, 0.25% Alg, 0.25% Alg –2% Gel, and 0.25% Alg–1% HA solutions treated with CAP for 10 min (CAP). Untreated (UT) sample for each condition was used as control. Each dot represents an independent sample measurement. Values represent mean ± SD. ***$p \leq 0.001$ and ****$p \leq 0.0001$.

3.2. Determination of the Tumor Weight and Percentage of Cancer Cells Population in Tumorsinici Del Formulari

To determine if CAP-treated hydrogels could reduce the tumors in the CAM model, we collected the tumors and weighed them 24 h after the last treatment. The results show no statistically significant differences between the tumor weight of untreated tumors and tumors treated with CAP-treated hydrogels or dH_2O (**Figure** 2A). Interestingly, we observed that tumors treated with CAP-treated Alg-HA presented a slight increase in the weight and size. To determine if this increase in tumor weight correlated with an increase in the number of cancer cells present in the tumor, we performed immunofluorescence staining for CD44, a specific stemness marker well expressed in Mia PaCa-2 cells and

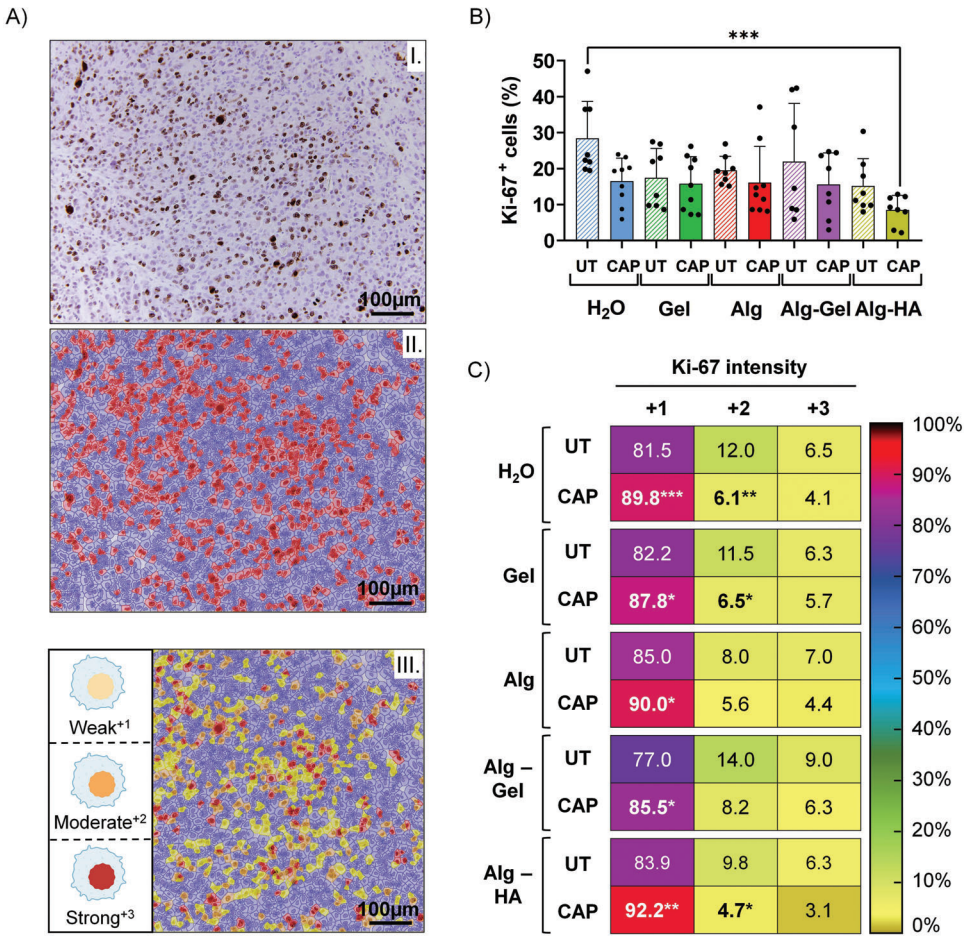

Figure 3. Identification of the proliferating cancer cells within the tumor and determination of their proliferating state. A) I) Representative image of Ki-67 immunohistochemical staining to visualize the proliferating Mia PaCa-2 cancer cells on tumor sections. II) Ki-67 positive Mia PaCa-2 cancer cells highlighted in red using the positive cell detection analysis from the Qupath software. III) Ki-67 positive Mia PaCa-2 cancer cells segregated into three different proliferating states through the application of different intensity thresholds using the QuPath software. The proliferating cells were scored as weak^{+1} (yellow), moderate^{+2} (orange), and strong^{+3} (red) proliferating states. Scale bar: 100 µm. B) Percentage of Ki-67 positive Mia PaCa-2 cancer cells within the tumor after three repeated exposures to dH_2O, 2% Gel, 0.25% Alg, 0.25% Alg–2% Gel, and 0.25% Alg–1% HA PTHs treated with CAP for 10 min (CAP). Untreated (UT) sample for each condition was used as control. Each dot represents an independent sample measurement. C) Percentage heat maps of the three different proliferating states scored in the tumor sections from all the studied conditions. Values represent mean ± SD. *$p \leq 0.05$, **$p \leq 0.01$ and ***$p \leq 0.001$.

PDAC.[28] Although larger, tumors treated with CAP-treated Alg-HA presented a significantly lower number of CD44$^+$ cells compared to the other CAP-treated tumors (Figure 2B), with fewer cancer cells in the proliferative front. To quantify this, we trained the object classifier in QuPath to discriminate human cancer cells from chicken cells (Figure 2C). The quantification demonstrated that indeed, CAP-treated Alg-HA tumors presented significantly lower percentages of cancer cells compared to the UT Alg-HA ($p \leq 0.001$) and the dH_2O controls ($p \leq 0.0001$; Figure 2D). We did not observe a variation in the number or distribution of Mia PaCa-2 cells in tumors treated with other hydrogels. These results indicate that CAP-treated Alg-HA can effectively reduce the overall population of cancer cells in the tumors, and the increase in tumor weight could be due to the infiltration of stromal cells from the chicken embryo.

3.3. Evaluation of the Proliferative State of Cancer Cells within Tumors

To further characterize the effect of CAP-treated hydrogels in in ovo tumors, we evaluated the expression of the proliferation marker Ki67 by immunohistochemistry. For this, we used a semi-automated analysis in QuPath to first identify the percentage of Ki67$^+$ cells and then classify the results based on the intensity of the signal of each cell. The results were scored as weak (+1), moderate (+2), or strong (+3) expression of Ki67 (**Figure 3A**). In general, CAP treatment showed a trend to reduce the expression of Ki67 in Mia PaCa-2 cells in in ovo tumors (Figure 3B). However, these differences were not statistically significant. Interestingly, CAP-treated Alg-HA tumors presented the least percentage of Ki67$^+$ cells. Further analysis of the intensity of

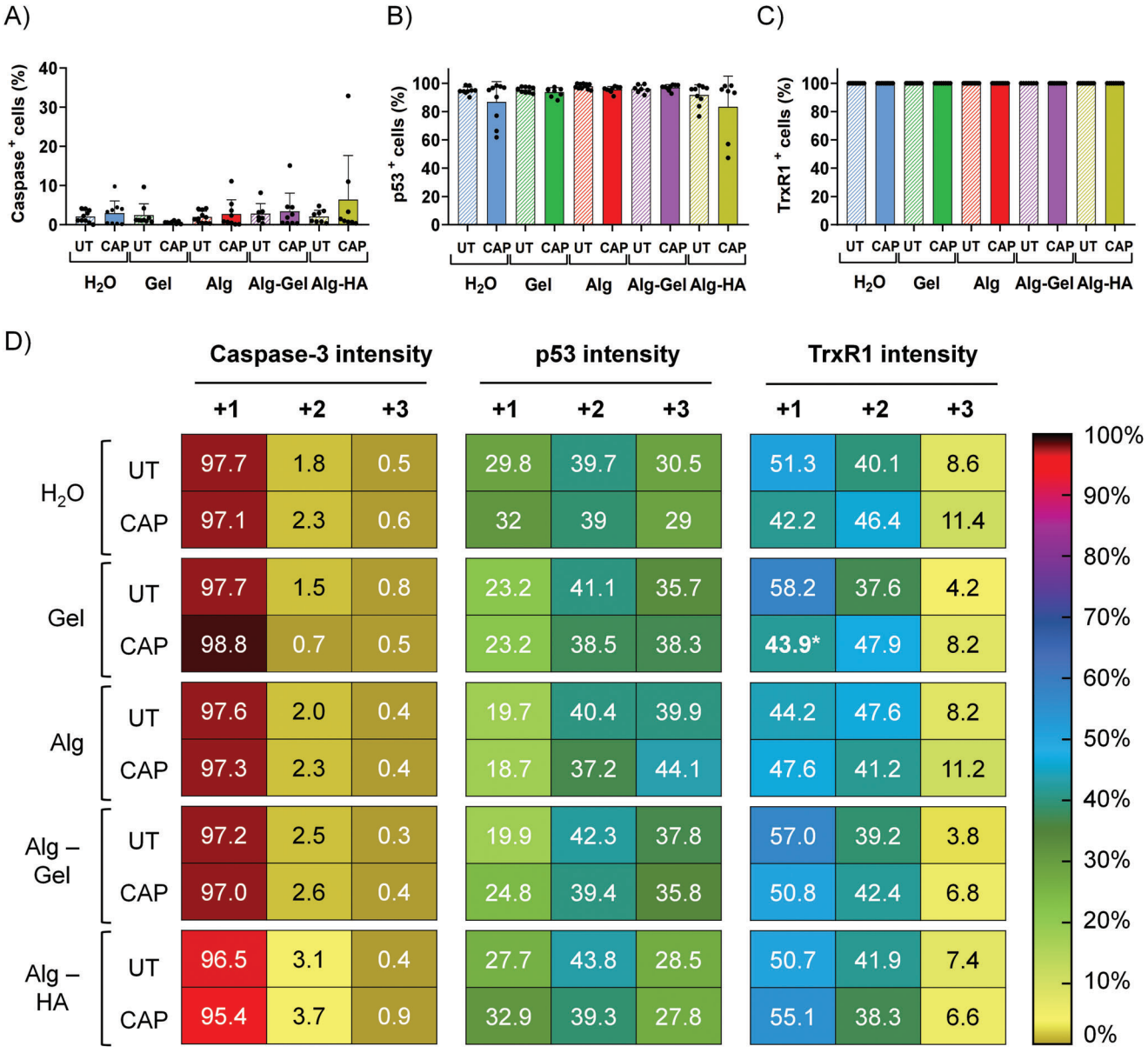

Figure 4. Immunohistochemical analysis of Caspase-3, p53, and TrxR1 biomarkers. Percentage of A) Caspase-3, B) p53, and C) trxR1 positive Mia PaCa-2 cancer cells within the tumor after three repeated exposures to dH_2O, 2% Gel, 0.25% Alg, 0.25% Alg–2% Gel, and 0.25% Alg–1% HA solutions treated with CAP for 10 min (CAP). Untreated (UT) sample for each condition was used as control. Values were obtained through the positive cell detection analysis from the QuPath software. D) Percentage heat maps of the three different expression degrees of caspase-3, p53, and TrxR1 biomarkers scored in the tumor sections from all the studied conditions. The different expression degrees were established through the application of different intensity thresholds using the QuPath software. Values represent mean ± SD. *$p \leq 0.05$.

Ki67 expression demonstrated that, in all cases, CAP treatment reduced the percentage of moderate (+2) and strong (+3) proliferating Ki67$^+$ cells in all scores, while increasing the percentage of weak (+1) proliferating cells (Figure 3C). CAP-treated Alg-HA tumors presented the lowest percentage of Ki67$^+$ cells (Figure 3B) and the highest fraction of weakly positive Ki67$^+$ cells (+1 score; $p \leq 0.01$), which could explain the low number of cancer cells found in the tumors (Figure 2B). Overall, these results suggest CAP-treated hydrogels, and especially CAP-treated Alg-HA, can reduce the expression of Ki67 in Mia PaCa-2 tumors in ovo.

3.4. IHC Analysis of Apoptosis and Oxidative Stress Biomarkers

To explore the mechanisms of cancer cell loss observed in CAP-treated Alg-HA tumors, we performed p53 and caspase-3 apoptosis immunohistochemical analyses. In both cases, the results show no statistically significant difference between the untreated and treated in ovo tumors, nor between the different CAP-treated hydrogels (**Figure** 4A,B,D). We also assessed the expression of thioredoxin reductase 1 (TxrR1), a regulator of the Nrf-Keap1 response axis involved in the antioxidant response. The results

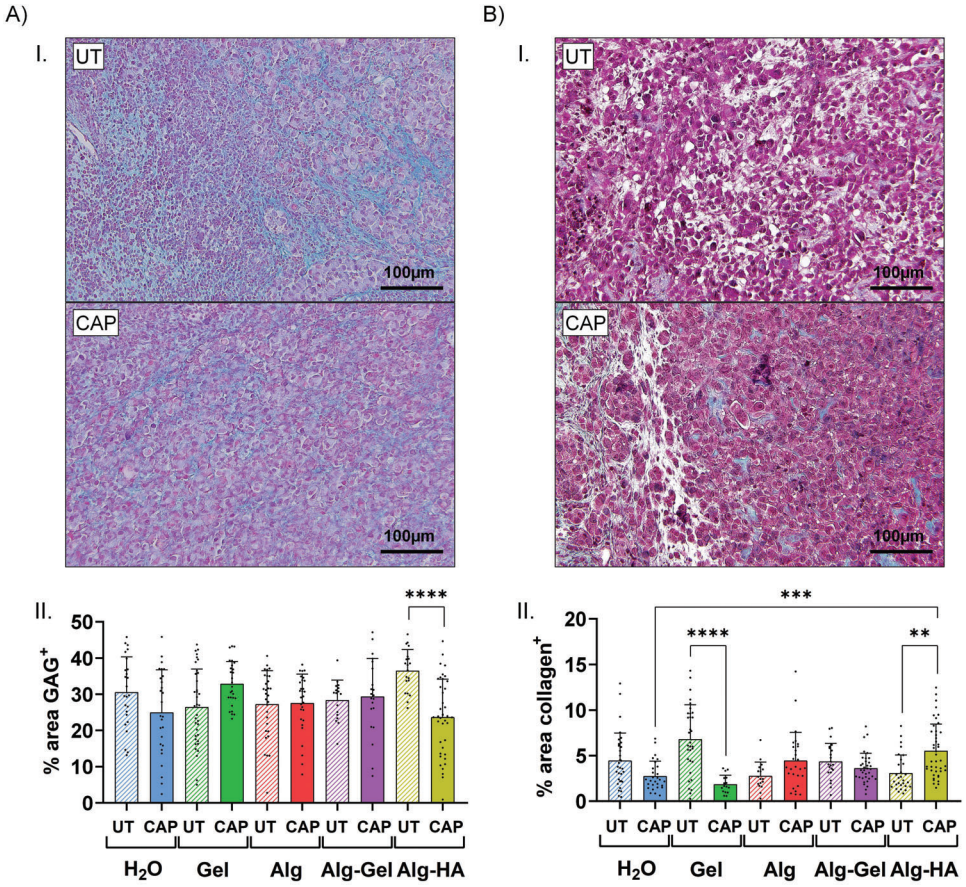

Figure 5. Evaluation of the extracellular matrix (ECM) composition. A) I) Representative images of Alcian Blue stains from histological sections of the tumors exposed to untreated (UT) and CAP-treated (CAP) 0.25% Alg–1% HA hydrogel treated with CAP for 10 min. II) GAGs (blue stained area in the Alcian Blue staining) of the tumors after three repeated exposures to dH_2O, 2% Gel, 0.25% Alg, 0.25% Alg–2% Gel, and 0.25% Alg–1% HA solutions treated with CAP for 10 min (CAP). Untreated (UT) sample for each condition was used as control. B) I) Representative images of Masson trichrome stains from histological sections of the tumors exposed to untreated (UT) and CAP-treated (CAP) 0.25% Alg–1% HA hydrogel treated with CAP for 10 min. II) Collagen (blueish/greenish stained area in the Masson trichrome staining) of the tumors after three repeated exposures to dH_2O, 2% Gel, 0.25% Alg, 0.25% Alg–2% Gel, and 0.25% Alg–1% HA solutions treated with CAP for 10 min (CAP). Untreated (UT) sample for each condition was used as control. Each dot represents an independent sample measurement. Values represent mean ± SD. $^{**}p \leq 0.01$, $^{***}p \leq 0.001$ and $^{****}p \leq 0.0001$.

showed that TrxR1 was well expressed in all cancer cells in the tumors (Figure 4C). CAP-treated hydrogels did not significantly affect the expression of this protein in cancer cells either, and only a small trend toward an increase in +2 and +3 $TrxR1^+$ cells was observed in CAP-treated dH_2O and Gel tumors (Figure 4D). Altogether, the results indicate that CAP-treated hydrogels at the plasma treatment time evaluated do not alter the activation state of p53, do not induce cell death via apoptosis, and do not increase the expression of TrxR1.

3.5. Evaluation of the ECM Composition of Tumors

To further determine the effect of CAP-treated hydrogels in other components of the tumor microenvironment, we explored the changes on the ECM components upon treatment. To this aim, we stained tissue sections with Alcian Blue and Masson's Trichrome to detect GAGs and collagen, respectively. Interestingly, CAP-treated Alg-HA tumors had a significant reduction in the % area of GAGs ($p \leq 0.0001$; **Figure** 5A) and an increase in the % area of collagen ($p \leq 0.01$; Figure 5B). In contrast, CAP-treated Gel tumors showed a reduction in the % area of collagen ($p \leq 0.0001$; Figure 5B).

Altogether, these results suggest that the type of hydrogel selected can alter the composition of the ECM, and that the reduction in the number of cancer cells in CAP-treated Alg-HA tumors observed in Figure 2 occurs in tumors with a decreased GAGs and increased collagen content.

3.6. Evaluation of the Internal and External Vascularization and Degree of Hypoxia of Tumors

Last, we assessed the vasculature of the CAM of the in ovo tumors to determine the role of CAP-treated hydrogels in the angiogenic process. The macroscopic assessment (**Figure** 6A) demonstrated that the application of hydrogels, CAP-treated or untreated, did not alter the number of small or large blood vessels branching out of the tumor (Figure 6B). In addition, the vascular network

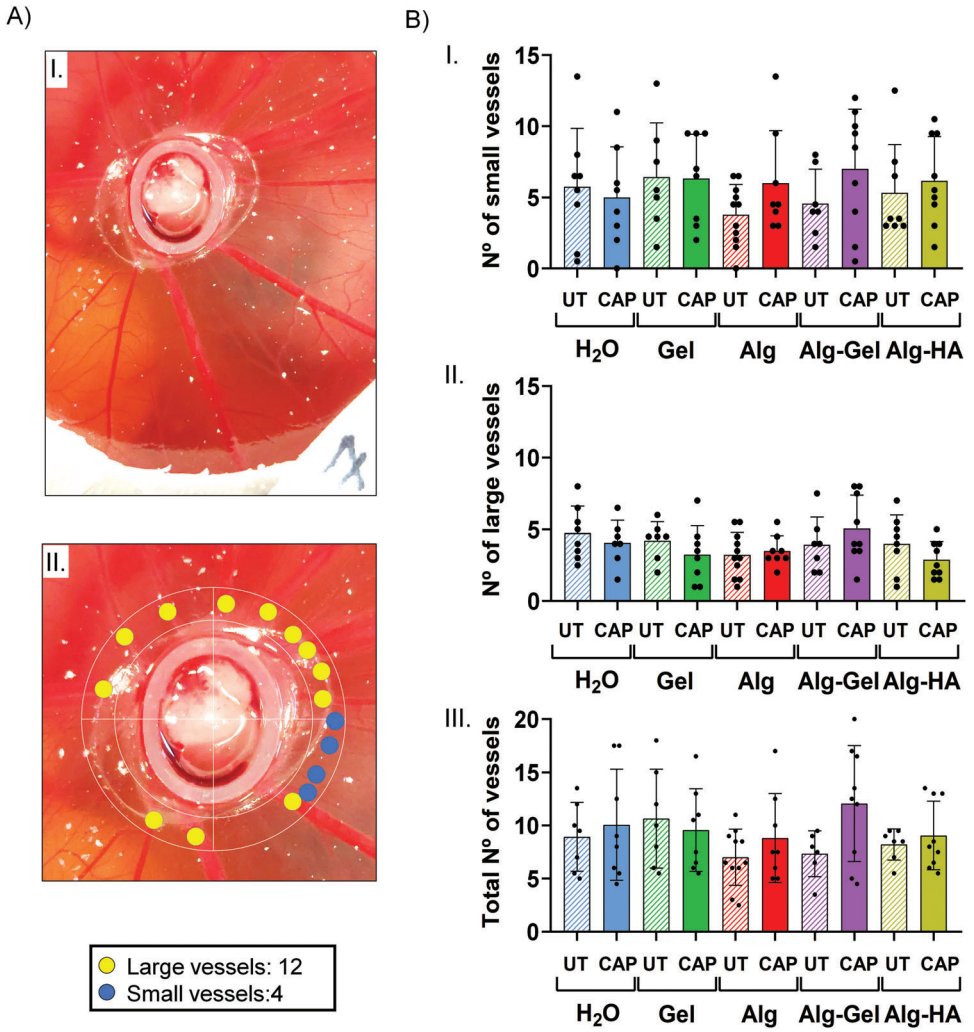

Figure 6. Evaluation of the external vascularization surrounding the tumors. A) I) Representative image of the external tumor vascularization employed for identification and counting of large (yellow dots) and small (blue dots) blood vessels. II) The spoke wheel pattern system employed to count the number of blood vessels intersecting the outer space of the two concentric circles. B) I) Small, II) large, and III) total number of blood vessels of tumors after three repeated exposures to dH_2O, 2% Gel, 0.25% Alg, 0.25% Alg–2% Gel, and 0.25% Alg–1% HA solutions treated with CAP for 10 min (CAP). Untreated (UT) sample for each condition was used as control. Each dot represents an independent sample measurement. Values represent mean ± SD.

surrounding the tumor was not different between the different hydrogels used.

We further determined the number of blood vessels within the tumor, both at the core and at the periphery (invasive front). Blood vessels were manually identified from H&E staining based on the presence of nucleated red blood cells from the chicken embryo, the presence of empty vessels surrounded by endothelial cells, or both (**Figure** 7A). The counting showed that there was a trend to lower blood vessel count in the core of Alg-HA tumors, especially after CAP treatment, compared to the other hydrogels (Figure 7B,C). However, these differences were not statistically significant. Altogether, these results suggest that the chosen hydrogels do not alter the angiogenic process of the CAM, and do not improve or hinder the blood vessels network within the tumors, thus also correlating with the absence of hypoxia in the CA IX staining (Figure 7D).

4. Discussion

Hydrogels, versatile materials with high water content and unique physicochemical properties, have emerged as promising tools in the field of cancer therapy. Recent advances, particularly those involving CAP technology, have further expanded the applications of hydrogels to address the limitations of current cancer treatments. In this work, we explored the use of hydrogels as a local delivery platform in cancer therapy. In particular, we investigated different hydrogel formulations involving Alg, Gel, and HA (Alg, Gel, Alg + Gel, and Alg + HA) and CAP-derived reactive species as anticancer agents through an in ovo pancreatic cancer model, shedding light on the potential advances of this evolving technology. In the first place, we conducted a chemical characterization of our formulations to know how CAP treatment affects the formulation's pH and to determine the

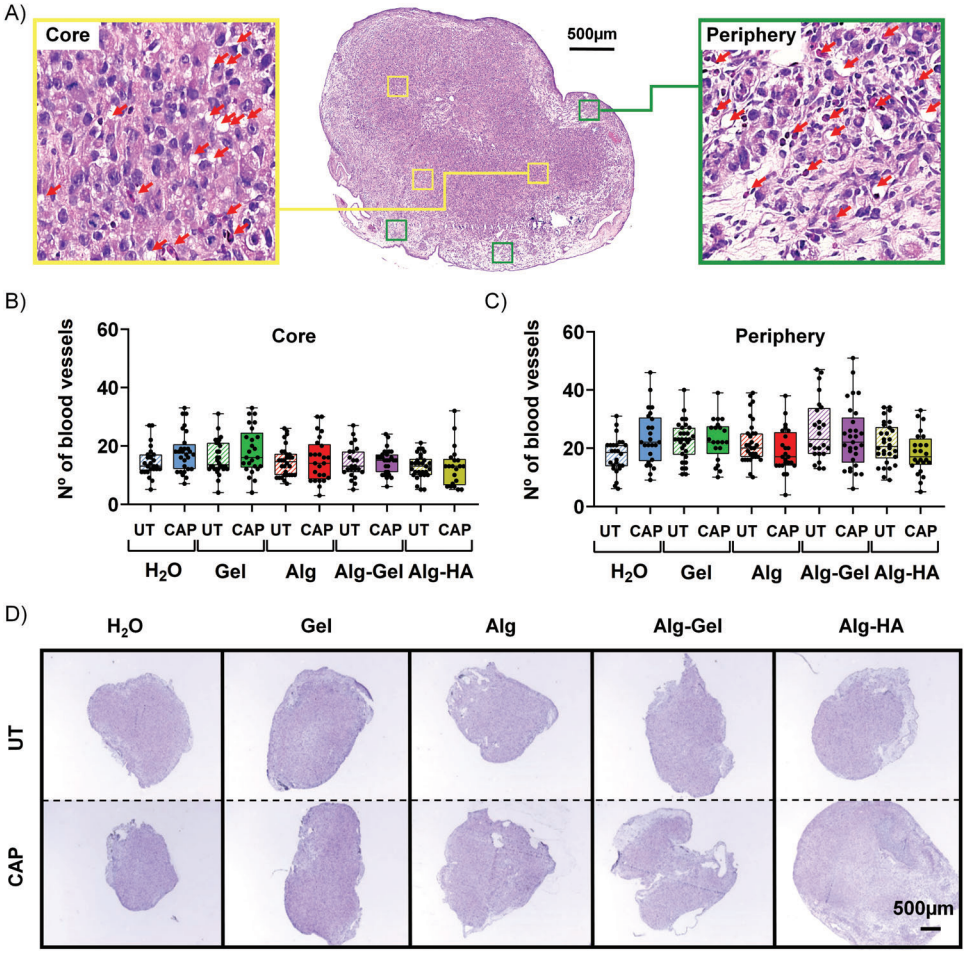

Figure 7. Evaluation of the internal microvasculature within the tumors and the degree of hypoxia. A) Image of a tumor section stained with Hematoxylin and Eosin, indicating the blood vessels counted in the core (red arrows) and periphery (red arrows). The regions to be counted were chosen randomly. Number of blood vessels counted in the B) core, and C) periphery of tumors after three repeated exposures to dH_2O, 2% Gel, 0.25% Alg, 0.25% Alg–2% Gel, and 0.25% Alg–1% HA solutions treated with CAP for 10 min (CAP). Untreated (UT) sample for each condition was used as control. Each dot represents an independent sample measurement. Values represent mean ± SD. D) Representative immunohistochemical staining of carbonic anhydrase IX (CA IX) to evaluate the hypoxic state of in ovo tumors after three repeated exposures to dH_2O, 2% Gel, 0.25% Alg, 0.25% Alg–2% Gel, and 0.25% Alg–1% HA solutions treated with CAP for 10 min (CAP). Untreated (UT) sample for each condition was used as control. Scale bar: 500 µm.

amounts of reactive species, H_2O_2 and NO_2^-, generated with a 10 min treatment. pH stability was observed around pH 6 for all formulations, while dH_2O showed a significant decrease from pH 6 to pH 4. These results align with literature demonstrating the buffering capacity provided by Alg and Gel in CAP-treated biopolymer solutions.[7,8] Ideally, when developing injectable formulations for drug delivery, it is recommended to maintain a pH close to the physiological level, ≈7, to reduce irritation and tissue damage.[29] Therefore, given that the pH of CAP-treated dH_2O was acidic, ≈4, the use of biopolymeric solutions/hydrogels with a pH ≈6 may offer a less aggressive option compared to dH_2O for delivering CAP-derived reactive species through direct injection on the tumor. In this sense, this approach could be considered for therapeutic strategies involving multiple injections. Regarding reactive species, H_2O_2 levels were similar in all biopolymeric formulations and dH_2O, with values ranging between 1200 and 1400 µM. However, for NO_2^-, dH_2O showed minimal presence, while biopolymeric solutions exhibited values ≈130–150 µM. The acidic pH-dependent transformation of NO_2^- to NO_3^- in dH_2O likely explains these differences.[5] Although H_2O_2 has been described as the main player in the cytotoxic activity of CAP-treated liquids, NO_2^- cannot be excluded from the equation as it was demonstrated to synergistically act together with H_2O_2 as anticancer agent.[30,31] For instance, Sardella et al. demonstrated that NO_2^- enhances the selective anticancer activity by decreasing the cytotoxic threshold of H_2O_2 on SaOS2 human osteosarcoma cancer cells, while maintaining a non-harmful threshold for the non-malignant EA.hy926 human endothelial cells.[32] Similarly, Bauer et al. described the molecular pathways behind the synergistic effects between H_2O_2 and NO_2^- to selectively trigger the mitochondrial pathway of apoptosis in MKN-45 human gastric adenocarcinoma cells.[33] Therefore, the different H_2O_2/NO_2^- balance in dH_2O, compared to biopolymeric formulations, should be taken into account to explain their biological effects in cancer cells.

After the chemical characterization, we evaluated the different formulations in an in ovo cancer model. Importantly, the administration of the hydrogels onto the tumors was applied through different strategies. Hydrogels based on Alg (Alg, Alg + Gel, and

Alg + HA) were directly injected/pipetted onto tumors, gellifying in situ. In contrast, Gel hydrogels were pre-gellified and then transferred on top of the tumors. These differences in the application arise from the distinct crosslinking mechanisms of Alg and Gel. Alg-based hydrogels solidify through ionic crosslinking with the addition of divalent ions like Ca^{2+}, enabling in situ crosslinking after injection[34] In contrast, Gel formulation relies on thermal crosslinking, solidifying at 4 °C and liquefying at 37 °C, allowing loaded compounds to be released upon contact with the human body, and also facilitating complete hydrogel degradation and absorption through physiological mechanisms.[35] Both administration methods allowed to successfully localize the PTH on top of the tumors. After the PTH treatments, we observed that the survival rate of the chicken embryos was 100%, highlighting the potential of the in ovo cancer model for developing and optimizing therapeutic approaches involving hydrogels as delivery platforms for anticancer drugs or bioactive agents in a cost-effective manner. In this study, none of the CAP-treated conditions were able to reduce the tumor mass. These results are not in accordance with what has been described in many publications, where the indirect CAP treatment has anticancer effects both in vitro and in vivo.[36] In this context, it is important to emphasize that often, when evaluating the therapeutic effect of a drug, the effects observed in in vitro studies do not replicate in in vivo models due to the complexity of the physiological microenvironment in vivo, which cannot be recapitulated in vitro[37] In this regard, the quantity and dosage of reactive species administered have been shown to determine the efficacy in terms of tumor mass reduction in vivo, which are significantly higher than the amounts of reactive species used in in vitro studies demonstrating anticancer effects.[38] In in vivo studies that successfully evaluate indirect treatment through CAP-treated liquids, the application of these liquids is usually prolonged over time through multiple injections, thus requiring large amounts of reactive species to obtain beneficial effects.[38] The need for high amounts of CAP-derived reactive species to achieve therapeutic effects when applied in more complex cancer models could explain our results. The high number of cancer cells within the tumor, the presence of ECM and the 3D scenario account for the higher resistance to RONS and the need for higher doses of RONS. Therefore, to achieve a reduction in tumor mass with our PTH, it would be necessary to optimize the treatment regime by increasing the CAP treatment time to enhance the quantity of reactive species in the hydrogels, and/or scheduling more administrations in the therapeutic plan. In the same line, the examination of the external and internal tumor vasculature did not reveal differences among all conditions. Neither reactive species generated with CAP in the dH_2O control and hydrogels, nor the biopolymers themselves of Alg, Gel, and HA promoted excessive blood vessel formation, which is crucial as vascularization promotion could lead to undesirable tumor growth. The formation of new blood vessels is essential for nutrient and oxygen supply during tumor development and growth. In this regard, it has been described that HA has influence on angiogenesis, promoting blood vessel formation via CD44 receptor interaction.[39] Therefore, the administration of HA might have resulted in detrimental effects with the formation of blood vessels in the tumor microenvironment. Luckily, in our study, we did not observe any enhancing effect of HA on blood vessel formation, neither at the level of macrovasculature surrounding the tumor nor of microvasculature within the tumor tissue, in line with the absence of hypoxia that we observed using the hypoxia marker CA IX.

Tumors were then analyzed in depth to ascertain any possible biological effect at cellular and microenvironmental level. To this end, histological sections were used to evaluate the cell populations present within the tumor, the proliferative state of cancer cells, and the induction of apoptosis and oxidative stress. The different cellular populations observed in the hematoxylin staining were identified and segregated using Qupath, thus determining the percentage of chicken and Mia PaCa-2 cancer cells within the tumoral tissue. All formulations exhibited similar percentages of cancer cells, except for CAP-treated Alg-HA, which showed a significant reduction in cancer cells. Possible explanations may involve again the CD44 cell surface receptor, a ligand for HA, which plays a key role in intracellular signaling pathways to promote angiogenesis, but also the survival and proliferation of cancer cells.[40] In this regard, Yusupov et al.[41] demonstrated that when HA is CAP-oxidized, the binding free energy of HA to CD44 decreases. Subsequently, it was observed that the reduction of HA-CD44 binding directly impacts several $CD44^+$ cancer cell types (U87-MG human glioblastoma, A375 melanoma, and HT29 colorectal cancer), resulting in a decreased proliferative state. In their study, it was also confirmed that the negative effect on the proliferative capacity of cancer cells is even higher when both HA and CD44 receptor are oxidized. In our approach the oxidation of both HA and CD44 receptor may occur; the HA may be oxidized during the CAP treatment, while the CD44 receptor of Mia PaCa-2 cancer cells within the tumor may be oxidized by the delivered CAP-derived reactive species. In this sense, the CAP-oxidized HA and/or CD44 receptor may inhibit/reduce the proliferative capacity of Mia PaCa-2 cancer cells. This hypothesis is supported by the significant downregulation of Ki67 proliferation marker upon CAP treatment. Moreover, the multi-intensity threshold analysis also indicated a shift from moderately and highly proliferative cells (Ki-67 +2 and +3) to a low proliferative state (Ki-67 +1), diminishing Mia PaCa-2 cancer cell proliferative capability.

In this context, to elucidate other possible mechanisms associated to the observed reduction of Mia PaCa-2 cancer cells, we assessed the expression of various biomarkers, including caspase-3 (apoptosis), p53 (cell cycle regulation), and TrxR1 (oxidative stress). However, no differences were observed among conditions for these biomarkers, suggesting minimal induction of apoptosis and oxidative stress. In contrast, some in vitro studies have demonstrated that CAP-treated liquids are able to induce cellular oxidative stress and cell death through apoptosis in Mia-Paca2 cancer cells. For instance, Sersenová et al.[42] showed that both CAP-treated medium and CAP-treated PBS could kill Mia Paca2 cells through caspase-3 dependent apoptosis. Similarly, Hattori et al.[43] stated that CAP-treated medium can induce caspase-3 guided apoptosis in Mia Paca2 cells by the generation of intracellular reactive oxygen species, induced by the oxidative stress resulting from the CAP-derived reactive species. All these in vitro studies were performed in 2D cell cultures, which, although they are the standard model for use in drug screening, do not accurately replicate the real tumoral microenvironment found in vivo,[44] which is challenging for CAP-treated liquids.[45] In this sense, the in ovo model recapitulates much better the

physiological conditions of tumors. This is because the tumor is fed through the vasculature from the chicken embryo, and the cancer cells are arranged in three dimensions within the ECM-like structure, allowing cell–cell and cell–ECM interactions.[21] Consequently, while in vitro studies demonstrate cancer cell death through the induction of oxidative stress and apoptosis by CAP-derived reactive species, when moving to the in ovo cancer model, the tumor mass is not reduced, and no signs of oxidative stress nor apoptosis are observed. This lack of effect would be probably attributed to the more complex microenvironment surrounding the cancer cells, which may provide protection against reactive species. This confirms that, increased doses of reactive species may be required to achieve effects comparable to those observed in in vitro studies.

Finally, we analyzed histological sections to determine the changes to ECM composition imposed by PTH. Notably, the evaluation of ECM indicated that HA had effects on GAGs and collagen levels in tumors. The untreated Alg–HA hydrogel showed similar GAGs values than the other conditions, however, when the CAP-treated Alg-HA hydrogel was applied, the content of GAGs within the ECM of the tumor was reduced. In contrast, the CAP-treated Alg-HA increased collagen levels in the tumor compared to its untreated counterpart. The HA is a natural GAG widely present in the ECM of human tissues and organs, including tumors, where it plays a key role in the biological function, structural integrity, and remodeling processes of the ECM.[46] However, depending on the context, it has been described that HA may promote opposite effects on many biological functions; for instance: anti- or pro-inflammatory and promoting or inhibiting cell proliferation and migration.[47] One possible mechanism behind these controversial effects is that the modification of the chemistry and/or macromolecular structure of HA may affect differently the HA-regulated pathways.[47] This could explain the opposite effects that we observed in the ECM composition, where the oxidation of HA by CAP inhibited the formation/deposition of GAGs, while promoting the production of collagen. In this sense, the administration of CAP-derived reactive species could also play an important role by inducing oxidative stress in the tumor ECM, potentially leading to the degradation of ECM components and affecting its structural integrity. Those changes in the ECM composition may be beneficial from the therapeutic point of view. HA is crucial in regulating the stiffness and permeability of the ECM. Due to its size and ability to form coils, HA can control the diffusion of biomolecules and ions throughout the ECM, thereby allowing small molecules to pass through the ECM, while blocking the transport or mobilization of larger molecules.[46] This combinatory effect of CAP-oxidized HA and reactive species could modulate the permeability of the tumor ECM to enhance drug penetration, facilitating the delivery of therapeutic agents to target cancer cells.

5. Conclusion

In this study, we validate for the first time the use of an advanced cancer in ovo model as a useful and cost-effective tool for developing and optimizing anticancer therapeutic approaches involving hydrogels as delivery platforms. In particular, in this work we employ the in ovo model to evaluate hydrogels based on Alg, Gel, and HA (Alg, Gel, Alg + Gel, and Alg + HA) for the delivery of CAP-derived reactive species as anticancer agents. In the first place, the chemical characterization showed that our PTH maintained a stable pH ≈6 in all different formulations, as well as, a similar production of reactive species (H_2O_2 and NO_2^-), compared to dH_2O where fewer NO_2^- were observed. After PTH treatment, the macroscopic assessment of tumors demonstrated that there were no significant differences between tumors treated with hydrogel formulations and the dH_2O control, both at the level of tumor mass and vascularization. However, at the microscopic level, a significant reduction in the population of $CD44^+$ cancer cells in the CAP-treated Alg-HA condition was observed, which correlated with a decrease in their proliferative state (ki67). The amount of CAP-derived reactive species administered through PTH and dH_2O treatment did not affect the expression of caspase-3, p53, and TrxR1, indicating the absence of apoptosis and cellular oxidative stress for the particular plasma treatment of 10 min. This indicates the need for optimizing the treatment regime by increasing the CAP treatment time to enhance the quantity of reactive species in the hydrogels and/or scheduling more administrations in the therapeutic plan to achieve the desired therapeutic effects. Last, we determined that the CAP-treated Alg-HA formulation affects the ECM composition, which could have implications for ECM stiffness and permeability and, which could be beneficial to enhance the therapeutic efficacy/uptake of anticancer drugs in combinatorial approaches. In conclusion, the combination of HA and oxidative stress derived from CAP through injectable Alg-based hydrogels presents a promising approach in cancer treatment. However, further research is needed, on the interaction between all bioactive components of this therapeutic approach and, on their influence on cancer cells and the tumor microenvironment, to better understand the potential benefits and risks, ultimately assessing their clinical impact.

Acknowledgements

The authors acknowledge the Instituto de Salud Carlos III (ISCIII) and the Next Generation EU funds through Project IHRC22/00003 SELLO EXCEL. ISCIII-HEALTH and MINECO for PID2022-141120OB-I00 funded by MCIU /AEI /10.13039/501100011033 / FEDER, UE. The authors belong to the SGR2022-1368. This research was partially funded by the Flanders Research Foundation, grant number G004524N (A.B. and A.P.-M.). Support for the research of C.C. was received through the ICREA Academia Award for excellence in research, funded by the Generalitat de Catalunya. The authors also thank COST Action CA20114 (Therapeutical Applications of Cold Plasmas) for the short-term scientific mission of Albert Espona-Noguera. Authors acknowledge Bioiberica S.A.U. for kindly providing Dermial.

Conflict of Interest

The authors declare no conflict of interest.

Data Availability Statement

The data that support the findings of this study are available from the corresponding author upon reasonable request.

Keywords

alginate, cancer, cold atmospheric plasma, hyaluronic acid, hydrogels

Received: June 4, 2024
Published online:

[1] L. Boeckmann, M. Schäfer, T. Bernhardt, M. L. Semmler, O. Jung, G. Ojak, T. Fischer, K. Peters, B. Nebe, B. Müller-Hilke, C. Seebauer, S. Bekeschus, S. Emmert, *Appl. Sci.* **2020**, *10*, 6898.
[2] A. K. Aranda-Rivera, A. Cruz-Gregorio, Y. L. Arancibia-Hernández, E. Y. Hernández-Cruz, J. Pedraza-Chaverri, *Oxygen* **2022**, *2*, 437.
[3] B. Perillo, M. Di Donato, A. Pezone, E. Di Zazzo, P. Giovannelli, G. Galasso, G. Castoria, A. Migliaccio, *Exp. Mol. Med.* **2020**, *52*, 192.
[4] G. Y. Park, S. J. Park, M. Y. Choi, I. G. Koo, J. H. Byun, J. W. Hong, J. Y. Sim, G. J. Collins, J. K. Lee, *Plasma Sources Sci. Technol.* **2012**, *21*, 043001.
[5] F. Tampieri, Y. Gorbanev, E. Sardella, *Plasma Process Polym.* **2023**, *20*, e2300077.
[6] X. Solé-Martí, T. Vilella, C. Labay, F. Tampieri, M.-P. Ginebra, C. Canal, *Biomater. Sci.* **2022**, *10*, 3845.
[7] M. Živanić, A. Espona-Noguera, H. Verswyvel, E. Smits, A. Bogaerts, A. Lin, C. Canal, *Adv. Funct. Mater.* **2023**, https://doi.org/10.1002/adfm.202312005.
[8] C. Labay, M. Roldán, F. Tampieri, A. Stancampiano, P. E. Bocanegra, M.-P. Ginebra, C. Canal, *ACS Appl. Mater. Interfaces* **2020**, *12*, 47256.
[9] F. Tampieri, A. Espona-Noguera, C. Labay, M.-P. Ginebra, M. Yusupov, A. Bogaerts, C. Canal, *Biomater. Sci.* **2023**, *11*, 4845.
[10] R. D. Kasai, D. Radhika, S. Archana, H. Shanavaz, R. Koutavarapu, D.-Y. Lee, J. Shim, *Int. J. Polym. Mater. Polym. Biomater.* **2023**, *72*, 1059.
[11] D. M. Rata, A. N. Cadinoiu, O. M. Daraba, L. M. Gradinaru, L. I. Atanase, D. L. Ichim, *Pharmaceutics* **2023**, *15*, 2240.
[12] M. Živanić, A. Espona-Noguera, A. Lin, C. Canal, *Adv. Sci.* **2023**, *10*, 2205803.
[13] P. Rosiak, I. Latanska, P. Paul, W. Sujka, B. Kolesinska, *Molecules* **2021**, *26*, 7264.
[14] A. Raslan, L. S. del Burgo, A. Espona-Noguera, A. M. O. de Retana, M. L. Sanjuán, A. Cañibano-Hernández, P. Gálvez-Martín, J. Ciriza, J. L. Pedraz, *Pharmaceutics* **2020**, *12*, 543.
[15] J. Alipal, N. A. S. Mohd Pu'ad, T. C. Lee, N. H. M. Nayan, N. Sahari, H. Basri, M. I. Idris, H. Z. Abdullah, *Mater. Today: Proc.* **2021**, *42*, 240.
[16] E. Ahmadian, S. M. Dizaj, A. Eftekhari, E. Dalir, P. Vahedi, A. Hasanzadeh, M. Samiei, *Drug Res.* **2020**, *70*, 6.
[17] A. Espona-Noguera, F. Tampieri, C. Canal, *Int. J. Biol. Macromol.* **2024**, *257*, 128841.
[18] M. Kapałczyńska, T. Kolenda, W. Przybyła, M. Zajączkowska, A. Teresiak, V. Filas, M. Ibbs, R. Bliźniak, Ł. Łuczewski, K. Lamperska, *Arch. Med. Sci.* **2018**, *14*, 910.
[19] J. Tornín, A. Villasante, X. Solé-Martí, M.-P. Ginebra, C. Canal, *Biol. Med.* **2021**, *164*, 107.
[20] M. Li, R. R. Pathak, E. Lopez-Rivera, S. L. Friedman, J. A. Aguirre-Ghiso, A. G. Sikora, *J. Vis. Exp.* **2015**, https://doi.org/10.3791/52411.
[21] L. Miebach, J. Berner, S. Bekeschus, *Front Immunol.* **2022**, *13*, 1006064.
[22] C. Labay, I. Hamouda, F. Tampieri, M.-P. Ginebra, C. Canal, *Sci. Rep.* **2019**, *9*, 16160.
[23] H. Zhang, S. Xu, J. Zhang, Z. Wang, D. Liu, L. Guo, C. Cheng, Y. Cheng, D. Xu, M. G. Kong, M. Rong, P. K. Chu, *Biomaterials* **2021**, *276*, 121057.
[24] P. Galvez-Martin, C. Soto-Fernandez, J. Romero-Rueda, J. Cabañas, A. Torrent, G. Castells, D. Martinez-Puig, *Int. J. Mol. Sci.* **2023**, *24*, 4774.
[25] J. Tornin, C. Labay, F. Tampieri, M.-P. Ginebra, C. Canal, *Nat. Protoc.* **2021**, *16*, 2826.
[26] P. Bankhead, M. B. Loughrey, J. A. Fernández, Y. Dombrowski, D. G. McArt, P. D. Dunne, S. McQuaid, R. T. Gray, L. J. Murray, H. G. Coleman, J. A. James, M. Salto-Tellez, P. W. Hamilton, *Sci. Rep.* **2017**, *7*, 16878.
[27] P. Hilkens, Y. Fanton, W. Martens, P. Gervois, T. Struys, C. Politis, I. Lambrichts, A. Bronckaers, *Stem Cell Res.* **2014**, *12*, 778.
[28] K. N. Sugahara, T. Murai, H. Nishinakamura, H. Kawashima, H. Saya, M. Miyasaka, *J. Biol. Chem.* **2003**, *278*, 32259.
[29] I. Usach, R. Martinez, T. Festini, J.-E. Peris, *Adv. Ther.* **2019**, *36*, 2986.
[30] E. Tsoukou, M. Delit, L. Treint, P. Bourke, D. Boehm, *Appl. Sci.* **2021**, *11*, 1178.
[31] J. Tornin, M. Mateu-Sanz, A. Rodríguez, C. Labay, R. Rodríguez, C. Canal, *Sci. Rep.* **2019**, *9*, 10681.
[32] E. Sardella, V. Veronico, R. Gristina, L. Grossi, S. Cosmai, M. Striccoli, M. Buttiglione, F. Fracassi, P. Favia, *Antioxidants* **2021**, *10*, 605.
[33] G. Bauer, *Redox Biol.* **2019**, *26*, 101291.
[34] A. Espona-Noguera, J. Ciriza, A. Cañibano-Hernández, L. Fernandez, I. Ochoa, L. S. del Burgo, J. L. Pedraz, *Int. J. Biol. Macromol.* **2018**, *107*, 1261.
[35] X. Jiang, Z. Du, X. Zhang, F. Zaman, Z. Song, Y. Guan, T. Yu, Y. Huang, *Front. Bioeng. Biotechnol.* **2023**, *11*, 1158749.
[36] J. Zhang, F. Li, K. Lu, W. Zhang, J. Ma, *Process Biochem.* **2023**, *131*, 77.
[37] H. Sajjad, S. Imtiaz, T. Noor, Y. H. Siddiqui, A. Sajjad, M. Zia, *Anim. Model. Exp. Med.* **2021**, *4*, 87.
[38] X. Solé-Martí, A. Espona-Noguera, M.-P. Ginebra, C. Canal, *Cancers* **2021**, *13*, 452.
[39] D. Park, Y. Kim, H. Kim, K. Kim, Y.-S. Lee, J. Choe, J.-H. Hahn, H. Lee, J. Jeon, C. Choi, Y.-M. Kim, D. Jeoung, *Mol. Cells* **2012**, *33*, 563.
[40] Z. Price, N. Lokman, C. Ricciardelli, *Cancers* **2018**, *10*, 482.
[41] M. Yusupov, A. Privat-Maldonado, R. M. Cordeiro, H. Verswyvel, P. Shaw, J. Razzokov, E. Smits, A. Bogaerts, *Redox Biol.* **2021**, *43*, 101968.
[42] D. Sersenová, Z. Machala, V. Repiská, H. Gbelcová, *Macromol. Chem.* **2021**, *26*, 4254.
[43] N. Hattori, S. Yamada, K. Torii, S. Takeda, K. Nakamura, H. Tanaka, H. Kajiyama, M. Kanda, T. Fujii, G. Nakayama, H. Sugimoto, M. Koike, S. Nomoto, M. Fujiwara, M. Mizuno, M. Hori, Y. Kodera, *Int. J. Oncol.* **2015**, *47*, 1655.
[44] F. Foglietta, R. Canaparo, G. Muccioli, E. Terreno, L. Serpe, *Life Sci.* **2020**, *254*, 117784.
[45] J. Tornín, M. Mateu-Sanz, V. Rey, D. Murillo, C. Huergo, B. Gallego, A. Rodríguez, R. Rodríguez, C. Canal, *Redox Biol.* **2023**, *62*, 102685.
[46] K. Dzobo, C. Dandara, *Biomimetics* **2023**, *8*, 146.
[47] S. Garantziotis, R. C. Savani, *Matrix Biol.* **2019**, *78*, 1.